ICAS 2016
30th Congress of the International Council of the Aeronautical Sciences
DCC, Daejeon, Korea ; September 25-30, 2016

CHARACTERISATION OF NS-DBD PLASMA ACTUATORS FOR SUPERSONIC FLOW CONTROL

Andrew Russell*, Hossein Zare-Behtash*, Konstantinos Kontis*
***University of Glasgow, School of Engineering, Glasgow, G12 8QQ, UK**

Keywords: *supersonic flow, flow control, energy deposition, plasma actuators*

Abstract

An experimental campaign was carried out to determine the efficacy of using infrared (IR) thermography to evaluate the electrical efficiency of nanosecond dielectric barrier discharge (NS-DBD) plasma actuators. The validity of this approach was proven using Schlieren photography. The effects on efficiency of various geometric parameters (anode width, cathode width and dielectric thickness) were then examined. It was shown, in line with previous results, that decreasing dielectric thickness results in more efficient actuators. The results for the anode and cathode widths were less conclusive and further studies need to be completed in order to provide more insight.

1 Introduction

NS-DBD refers to nanosecond dielectric barrier discharge plasma actuators. The dielectric barrier discharge effect was first discovered in 1857 [1] and refers to the electrical discharge that occurs between two electrodes separated by an insulating, dielectric barrier. The use of dielectric barrier discharge plasma actuators as a means of flow control has been studied since 1998.[2] There are two types of DBD plasma actuators: AC and NS. The two prefixes refer to the type of supply voltage signal used to drive them. In this study the interest is in the nanosecond (NS) plasma actuators. These function by using rapid localised heating to generate pressure waves.[3] These pressure waves are the means by which the actuators can control high speed flows. One area of particular interest is supersonic and hypersonic transport aircraft.

There are still many challenges to overcome for supersonic/hypersonic transport aircraft. One of the key issues is the efficiency/reliability of the propulsion systems.[4] A phenomenon observed in ramjets/scramjets, the most widely studied high speed propulsion systems, is unstart. This is the ejection of the shock structure that forms inside the engine intake, a shock train, upstream of the inlet.[5 ,6] It is proposed that the application of NS-DBD plasma actuators within the intake geometry could mitigate the effect of this and improve reliability and efficiency of the propulsion system intake[4].

If these flow control devices are to be used in real-world applications, as with any technology, efficiency is an important consideration. There are many ways to define efficiency, the global efficiency would in this case relate the improvement in system performance compared to the required energy input to achieve this improvement. However, as a first step to being able to evaluate the global efficiency this study looks to determine the effect of different actuator geometric parameters on the ‘electrical conversion efficiency’. This refers to how well the actuator transforms electrical energy into useful work done to the flow, the rapid heating of the air to create pressure waves. This is done by measuring the surface temperature with the actuator turned on to allow the loss through the dielectric barrier to be calculated.[7]

2 Experimental Setup

2.1 NS-DBD Plasma Actuator Models and Design Parameters Investigated

This study will examine the impact that three different geometric variables have on actuator efficiency: anode width, cathode width and electrode length. Future work will go on to examine further variables such as supply voltage, supply frequency and supply pulse polarity. This study was carried out at a supply voltage and frequency of 12kV and 1 kHz respectively.

The actuators are made through the process of double-sided photolithography. The masks for the process were created using SolidWorks to ensure their accuracy as much as possible. The reason for using this production mechanism instead of the more common method of producing them by hand is for accuracy and repeatability. This method allows the actuators to be made to the exact dimensions desired and so any results from the characterisation can be relied upon when actuators are used for future experiments.

Table 1 shows the values tested for each parameter.Figure 1 shows a simple diagram of an actuator and highlights what each of the geometric parameters in Table 1 refer to. It also highlights the values that are present for the baseline 'control' case. This is the case that is part of every dataset and uses the 'standard' values for each variable, i.e. for the anode width test cases, the cathode width and electrode length are the same as that of the baseline case.

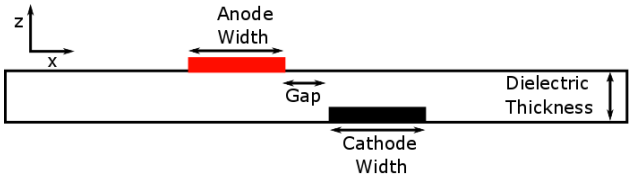

Figure 1 - Diagram of NS-DBD actuator

Geometric Parameter	Values (mm)
Anode width	2, **5**, 10, 20
Cathode width	5, **10**,15, 20, 30, 40
Dielectric thickness	0.4, 0.8, **1.6**

Table 1 - Values tested for each geometric parameter examined (values in bold are the baseline 'control' actuator)

2.2 Infrared (IR) Thermography and Inverse Heat Transfer Problem (IHTP)

2.2.1 IR Thermography

For this study IR images are required for each of the test cases (described in Table 1) that are to be examined. These images are captured using a FLIR A655sc thermal imaging camera. The camera has a maximum resolution of 640 x 480 pixels. However the actual resolution used was limited to 640 x 240 due to using a higher frame rate of 100Hz to capture images.

NS-DBD plasma actuators and the associated high voltage generators themselves generate electromagnetic interference (EMI). It was found that this had a significant effect on the IR camera's operation. To reduce the impact of the EMI the camera was placed inside a Faraday cage to shield the camera from the majority of this radiation.

2.2.2 IHTP

The IR images captured are then used to calculate the heat flux through the dielectric material i.e. the rate of energy being lost due to conduction through the dielectric barrier of the actuator. One of the main assumptions for this study is that the only significant source of loss is that associated with conduction through the dielectric barrier. The orientation of the actuator ensures that there are negligible losses from convection. Other sources of loss such, as radiation for example, are also assumed to be negligible.

Based on these assumptions an IHTP is solved based on the temperature profiles captured by the IR camera. The temperature profile used is an average over the length of the actuator. This allows the heat flux to be calculated for each pixel location along the length of the discharge. The discharge length is determined through inspection of the temperature maps from the IR camera. This temperature profile is then used to solve for the heat flux at each pixel location for each time step, based on the boundary conditions given by:

$$\frac{\partial T}{\partial t} = \alpha \frac{\partial^2 T}{\partial z^2} \qquad (1)$$

$$q_z = k\frac{\partial T}{\partial z} \quad (2)$$

$$T_0(\in x_s, \in y_s) = T(\in x_u, \in y_u) = T_{init} \quad (3)$$

where T is surface temperature, z is the coordinate in the z-direction (perpendicular to the actuator surface, seeFigure 1), α is the thermal diffusivity of the dielectric, q_z is heat flux in the z-direction, and the subscripts s and u refer to the discharge surface and the underside of the actuator respectively.

This methodology assumes that the temperature on the underside of the actuator is constant throughout the measurements. Theoretically this is valid if the dielectric thickness is larger than the penetration depth:

$$d_p = 4\sqrt{\alpha t} \quad (4)$$

where d_p is the penetration depth and t is time. However, from examining the data from the IR camera, the length of time for which this assumption is valid for is larger than that suggested by the theoretical equation (0.0548s) for the thinnest sample. It holds valid for a minimum of 0.15s, the maximum time over which data is collected. Therefore the constant temperature assumption on the underside of the actuator is deemed to be acceptable.

The heat flux is solved in an iterative manner using the boundary conditions described above. This is done by comparing the difference between the experimental temperature profile and the temperature profile obtained using the current value of the heat flux. The value of heat flux is then altered using the optimisation toolbox in MATLAB to minimise the difference in the two profiles.

2.3 Schlieren Photography

Schlieren photography is a well-established imaging technique used to visualise high density gradients. A Photron SA-1 camera was used to capture the Schlieren images. A z-type Schlieren system was used, similar to that of Gnani et al.[8] The pressure waves generated by NS-DBD plasma actuators exhibit such density gradients. Here the technique will be used to provide a measure of the pressure wave strength. This will act as a form of validation for the IR imaging measurement technique. The current assumption is that all the actuators used have an equal impedance**.** Therefore the energy supplied to each actuator should be equal, as the ratio of supplied to reflected energy back down the transmission line is dependent on the relationship between the impedance of the actuator and the generator. This assumption leads on to the conclusion that a more efficient actuator supplied with the same energy should create a stronger pressure wave. Therefore if Schlieren imaging can show this is the case for the more efficient actuators it will go some way to validating the IR imaging measurement technique.

3 Results

3.1 IR Thermography and IHTP

MATLAB is used to determine the heat flux for each actuator based on the temperature profile obtained from the IR camera. An example of the temperature profile at a single point throughout the discharge is shown in Figure 2 and an example of the temperature profile along the plasma at one time step is shown Figure 3. These profiles show the temperatures obtained for a single point and a single section through the plasma respectively. For the heat flux calculation, values are calculated at each point along the discharge over a section of the anode length. The final heat flux value for each actuator is then calculated as a sum of these values based on plasma area and length.

The results of the IR thermography and IHTP are shown in Figure 4. Each actuator is represented as a single point as each actuator has a single value for heat flux.

Examining the results Figure 4 it can be seen that the trend in heat flux when the dielectric thickness is altered is the same trend as in the previous work of Avallone et al.[7] and Broeke et al.[9] This suggests that the IR measurements and IHTP solver functioned as intended. Examining the further test cases presented, anode

and cathode width, does not immediately show any obvious trends as with the dielectric thickness cases. However future work, implementing the electrical measurements to complement the thermography results, will provide more conclusive results. The only concern with the current thermographic results is the accuracy of the equipment used. This does not cause any issue with the dielectric thickness case as the temperature changes measured are significant. However, as demonstrated by the significantly smaller heat flux values, for the other cases the temperature changes are smaller.

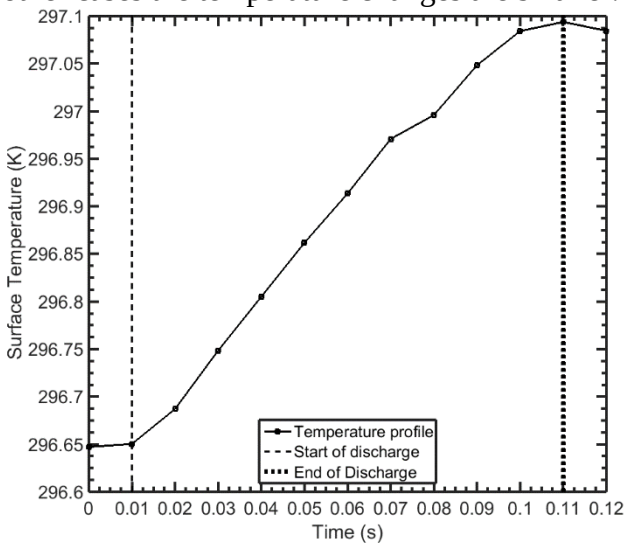

Figure 2 - Temperature profile at the edge of the anode throughout the discharge

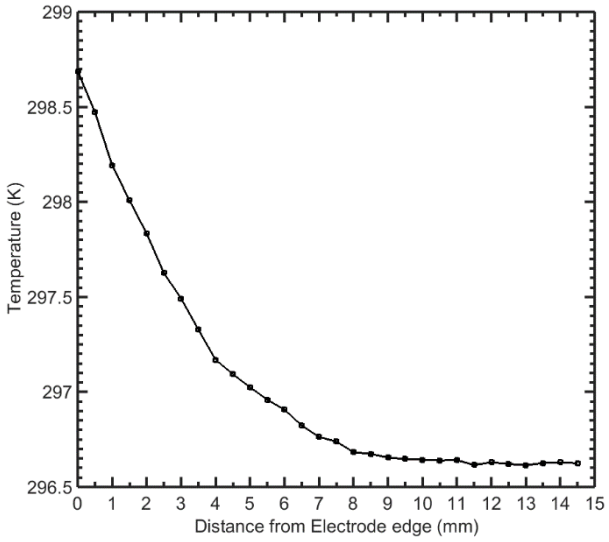

Figure 3 - Temperature profile along the plasma discharge region at the end of the discharge (t = 0.11s)

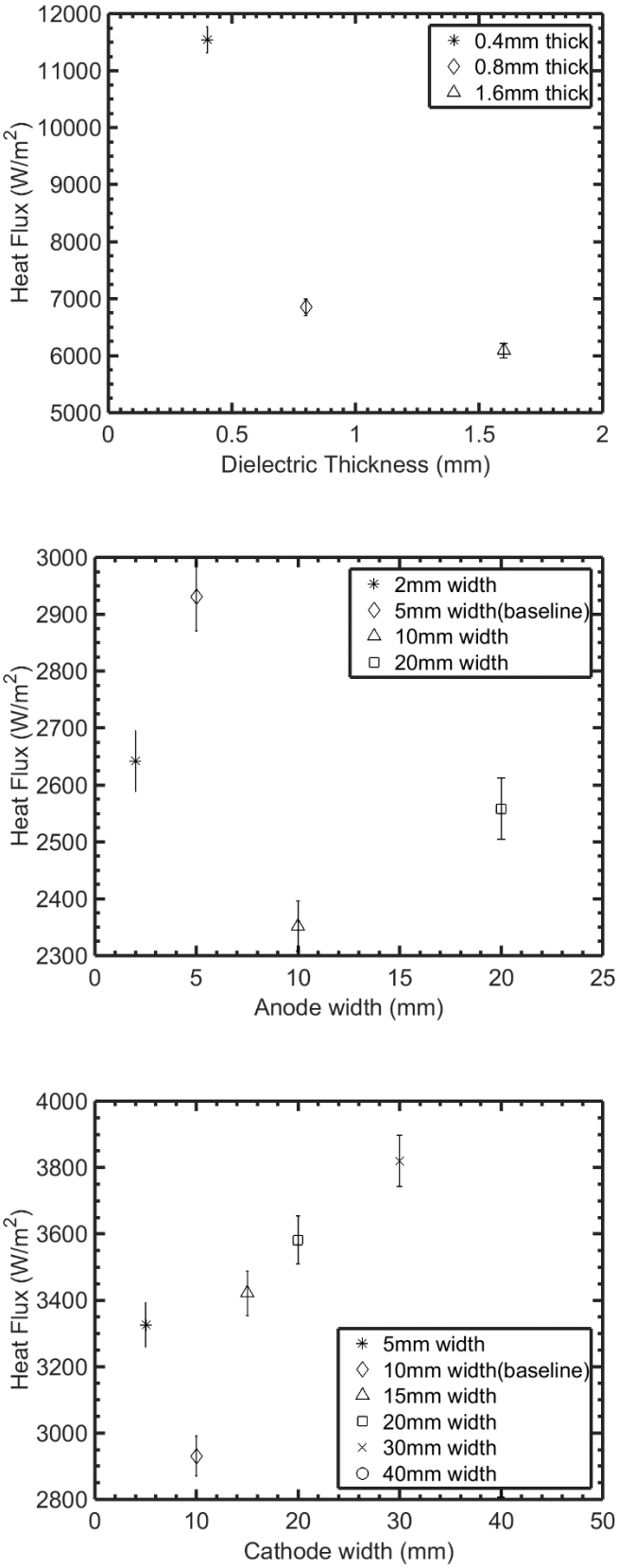

Figure 4 - Effect on Heat flux calculated from IR imaging of the following geometric parameters (from top to bottom): dielectric thickness, anode width and cathode width

3.2 Schlieren Photography

Schlieren images were captured for each actuator in an attempt to validate the IR thermography approach. The images were taken along the length of the actuator where possible. This increased the signal to the camera as the wave seen was a result of line-of-sight averaging along the actuator. However this could not be done for the actuators where the length is altered as this would affect the 'quantitative' results taken from them. Therefore for the cases where length is altered the images are taken across the electrode.

An example of the Schlieren images captured is shown in Figure 5. Each wave image used to extract values for shock strength is obtained by phase-averaging the images over the course of the run. Each image containing a pressure wave is then normalised by a background, phase-averaged image taken from each run. An example of the resulting normalised intensity profile is shown in Figure 6**.** The peak locations marked in this figure are those used in Figure 7 to display the variation in shock strength with the geometric parameters investigated.

An examination of Figure 7 shows that the trend for shock strength when dielectric thickness is altered is consistent with that of the heat flux from the IR measurements. The IR measurements match those of previous studies [7,9] indicating that decreasing dielectric thickness does increase efficiency. With decreasing dielectric thickness the shock strength is also increased. This is intuitive as the more efficient the actuator, a larger percentage of the electrical energy that is converted to thermal energy resulting in a stronger pressure wave.

The results of the other investigated parameters are less conclusive. This is due to the increasing percentage of uncertainty in the IR measurements observed as the maximum temperature (and thus calculated heat flux) decreases. As a result, conclusions are more difficult to draw from the results of the anode and cathode widths. However, it is expected that there are trends to be observed in the relationships between actuator efficiency and anode/cathode width if the uncertainty in the IR measurements could be reduced.

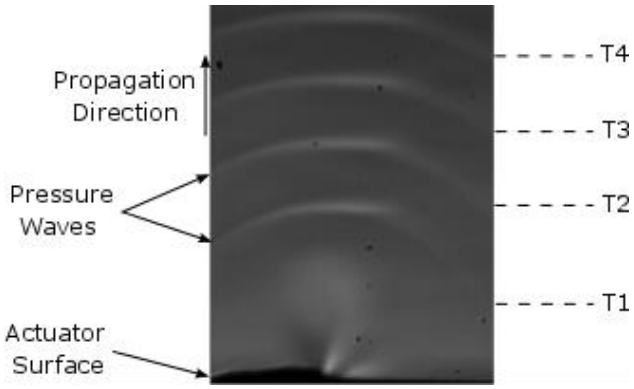

Figure 5 - Schlieren images from one test case superimposed to show progression of pressure wave in time

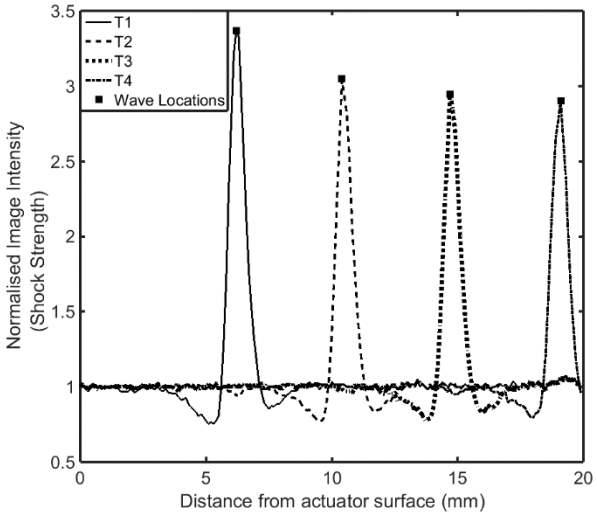

Figure 6 - Normalised image intensity illustrating peak intensity locations for each pressure wave image

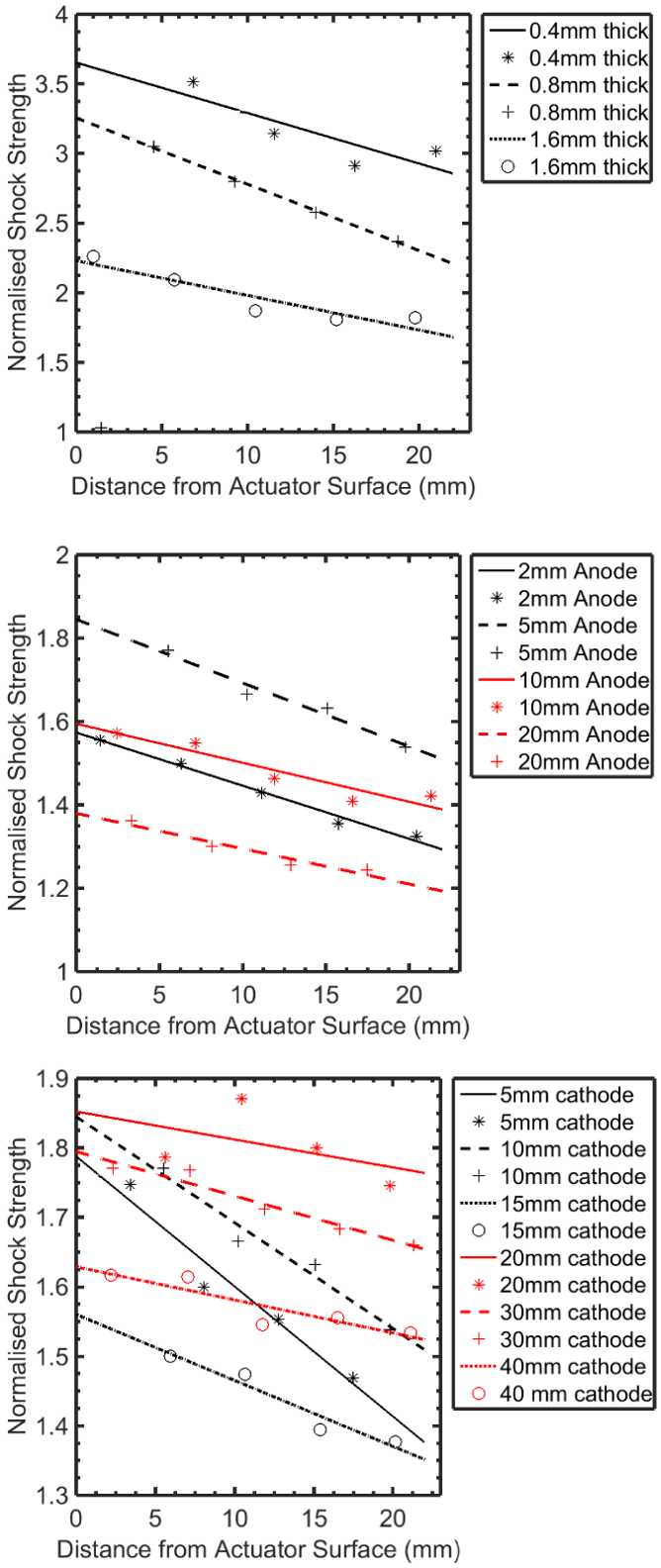

Figure 7 - Effect on Shock strength calculated from Schlieren imaging of the following geometric parameters (from top to bottom): dielectric thickness, anode with and cathode width.

4 Conclusions

The primary aim of this study was to investigate the validity of using infrared thermography while the secondary aim was to implement this technique to optimise NS-DBD plasma actuators.

The trends of the heat flux from IR measurements with the shock strengths results from the Schlieren experiments were compared. This along with comparison of the current work with previous studies presents convincing evidence that IR thermography can be used to investigate effectively the efficiency and, by association, the resulting pressure wave strength of NS-DBD plasma actuators.

The results of the secondary were also promising but require further investigation to be fully understood. Initial results suggest that there is still correlation between the IR and Schlieren results when the temperature differences are smaller (as with the other test cases). However the level of accuracy of the equipment, the IR camera, starts to become an issue. This will continue to be examined in the future along with the implementation of electrical measurements to complement these results.

5 Contact Author Email Address

For any queries regarding the work please contact a.russell.2@research.gla.ac.uk.

References

[1] Siemens W. Ueber die elektrostatische Induction und die Verzogerung des Stroms in Flaschendrahten. *Poggendors Annalen der Physik und ChemieSmith*, 1857.

[2] Roth J R, Sherman D M, Wilkinson S P. Boundary layer flow control with a one atmosphere uniform glow discharge surface plasma. *Aerospace Sciences Meeting and Exhibit*, Reno, Vol. 36, 328, pp 1-28, 1998.

[3] Roupassov D V, Nikipelov A A, Nudnova M M, Starikovskii A Y. Flow separation control by plasma actuator with nanosecond pulsed-periodic discharge. *AIAA Journal*, Vol. 47, No. 1, pp 168-185, 2009.

[4] Russell A, Zare-Behtash H, Kontis K. Joule heating flow control methods for high-speed flows. *Journal of Electrostatics*, Vol. 80, pp 34-68, 2016.

[5] Emami S, Trexler C A, Auslender A H, Weidner J P J. Experimental investigation of inlet-combustor

isolators for a dual-mode scramjet at a Mach number of 4. *Technical Report*, 1995.

[6] Wagner J L, Yuceil K B, Clemens N T. Velocimetry measurements of unstart of an inlet-isolator model in Mach 5 flow. *AIAA Journal*, Vol. 48, No. 6, pp 1875-1888, 2010.

[7] Avallone F, Correale G. Method to quantify the electrical efficiency of a ns-DBD plasma actuator. *Pacific Symposium on Flow Visualization and Image Processing.* Vol. 10, pp 1-10, 2015

[8] Gnani F, Lo K H, Zare-Behtash H, Kontis K. Shock wave diffraction in the presence of a supersonic co-flow jet. *Shock Waves*, Vol. 26, pp 253-262, 2016

[9] Broeke V J, Correale G, Avallone F. A Characterization study on the electrical and fluid-mechanical efficiency of the nanosecond-pulsed dielectric barrier discharge plasma actuators. *AIAA Aerospace Sciences Meeting*, Vol. 54, pp 1-16, 2016.

Copyright Statement